On the enzymatic activity of catalase: an iron L-edge X-ray absorption study of the active centre†

Nora Bergmann,[a] Sébastien Bonhommeau,[b] Kathrin M. Lange,[c] Stefanie M. Greil,[c] Stefan Eisebitt,[cd] Frank de Groot,[e] Majed Chergui*[f] and Emad F. Aziz*[cf]

Received 17th November 2009, Accepted 10th February 2010
First published as an Advance Article on the web 16th March 2010
DOI: 10.1039/b924245g

Catalase and methaemoglobin have very similar haem groups, which are both ferric, yet catalase decomposes hydrogen peroxide to water and oxygen very efficiently, while methaemoglobin does not. Structural studies have attributed this behaviour to their different distal environments. Here we present Fe $L_{2,3}$-edge X-ray absorption spectra of these proteins in physiological solutions, which reveal clear differences in their electronic structures, in that π back-donation of the Fe atom occurs in catalase, which confers on it a partial ferryl (Fe^{4+}) character, while this is not the case in methaemoglobin. The origin of the Fe^{4+} character stems from the proximal tyrosine residue. We also find that both systems are in a high spin state. Temperature effects influence the spectra of catalase only weakly, in agreement with previous studies of its chemical activity. We conclude that the high activity of catalase is not only determined by its distal environment but also by its partial ferryl character.

1. Introduction

Catalase is a common enzyme found in nearly all living organisms exposed to oxygen. As with methaemoglobin (metHb), it is a tetramer whose monomer units are haem proteins with a ferric active centre. Catalase plays an important role in the defence of aerobic organisms against oxidants[1] as it converts two molecules of hydrogen peroxide into water and oxygen *via* a 2-step reaction cycle, in which the substrate alternately acts to oxidize and then reduce the haem iron. This activity has one of the highest turnover numbers of all enzymes: one molecule of catalase can convert up to 10^6 hydrogen peroxide molecules to water and oxygen per second.[1] Surprisingly, metHb, which is in a high spin (HS) state,[2] carries out this function with a much lower efficiency. This is also the case with myoglobin (Mb), which is a monomer that is structurally very close to Hb monomers.[3] Contrary to catalase, the reaction of Hb and Mb with peroxide is non-enzymatic, as they are altered through repeated cycles.[4]

Structurally, metHb and catalase show major differences. While both have the haem group located at the surface of their monomer units, in Hb, the surface is exposed to the solvent, while in catalase it is positioned inside the tetramer so that relatively long channels lead to the haem moiety. Another important difference between globins (Hb, Mb) and catalases is that in the former, the proximal residue is histidine (His), which provides the only linkage from the haem to the protein backbone *via* a nitrogen atom, while in catalases it is tyrosine (Tyr). In haem enzymes such as peroxidases, which function similarly to catalases, the proximal residue is His in horse radish peroxidase or cytochrome c peroxidase, but is a cysteine in peroxidase 450 (P450). Furthermore, the distal environment is also different: the nearest residues are His and/or arginine (Arg) and/or tryptophan (Trp) in globins and peroxidases, but in catalase consists of asparagine (Asn) and His.

The formation of so-called compound I, which is an oxyferryl (iron in the Fe^{4+} state bound to an oxygen atom), initiates the activity of catalases and peroxidases.[5] In this contribution, we address the causes of its formation, which underlie the different activities of catalases and globins. Structural studies have addressed the activity of catalases, peroxidases and globins by X-ray crystallography[1,4,6–11] and X-ray absorption spectroscopy (XAS) at the K-edge of iron (~7.2 keV). XAS provides information about the number and average distance of the ligand atoms around Fe *via* analysis of the extended X-ray absorption fine structure (EXAFS) and X-ray absorption near edge structure (XANES). The latter also provides information about the electronic structure *via* the pre-edge 1s–3d quadrupole transition features, which become partly allowed due to the ligand field around the Fe atom. For catalases, the XAS studies performed so far have concerned the protonated oxyferryl form (*i.e.*, with OH ligated to Fe^{4+}) and not the resting form, which has a water molecule ligated to Fe^{3+}.[12]

[a] *Max-Delbrück-Center for Molecular Medicine, D-13125 Berlin-Buch, Germany*
[b] *Institut des Sciences Moléculaires-UMR 5255 CNRS, Université Bordeaux 1, 351 cours de la Libération, 33405 Talence Cedex, France*
[c] *Helmholtz-Zentrum Berlin für Materialen und Energie c/o BESSY II, Albert-Einstein Strasse 15, 12489 Berlin, Germany. E-mail: Emad.Aziz@helmholtz-berlin.de*
[d] *Technical University Berlin, Institute for Optics and Atomic Physics ER 1-1 Strasse des 17. Juni 135, 10623 Berlin, Germany*
[e] *Department of Inorganic Chemistry and Catalysis, Utrecht University, Sorbonnelaan 16, 3584 CA Utrecht, The Netherlands*
[f] *Ecole Polytechnique Fédérale de Lausanne, Laboratoire de Spectroscopie Ultrarapide, Faculté des Sciences de Base, ISIC-BSP, CH-1015 Lausanne-Dorigny, Switzerland. E-mail: Majed.Chergui@epfl.ch*
† Electronic supplementary information (ESI) available: Further experimental details. See DOI: 10.1039/b924245g

The effect of temperature on the enzymatic activity of catalases was investigated by different methods and was reported to be weak. Interestingly Bragger *et al.*[13] found no change of activity (after correcting for solvent fluidity and diffusion of the substrate) down to −100 °C, *i.e.*, to temperatures below the dynamic transition for proteins. This suggests that protein motions, which are then frozen, are not essential for enzyme activity. Shi *et al.*[14] and Haber *et al.*[15] have also reported no change of enzymatic activity in the 25–40 °C range at pH 7.0.

While a fairly clear picture is available of the global structure of the proteins, of their haem environment (distal and proximal) and of the porphyrin itself, the connection to the high activity of the active centre of catalases is still not clear. The Fe valence d-orbitals are those involved in the binding to the porphyrin, to the axial amino acid residues and to the substrate ligand. As a result, their energetics, ligand-field splittings and spin states are strongly affected by the environment and, in particular, by the proximal residue. The best way to visualize the electronic structure of haem and non-haem Fe-complexes is by soft XAS at the $L_{2,3}$-edges (which stem from the $2p_{1/2,3/2}$ core levels) of the Fe atom.[11,16–20] Compared to the K-edge spectroscopy previously used,[21] the allowed p–d transitions of the metal are characterized by sharp spectral features, since the core hole lifetime width is significantly lower.

Because of the large absorption cross-section of solvents and air (*e.g.*, in the Fe L-edge energy range, the X-ray path length in water is only 1–2 μm), the implementation of soft XAS of high vapour-pressure solutions was hampered for a long time because of the need for a high vacuum. However, in the last few years, these problems have been overcome by the use of high speed liquid jets or of flow cells equipped with soft X-ray transparent ∼100 nm-thick silicon nitride membrane windows, opening the way to studies of chemical systems in solution.[22] We recently extended these studies to proteins in physiological solutions and recorded the Fe L-edge spectra of haemoglobin and hemin.[2] The issue of radiation damage was critical, and the solutions had to be renewed by continuous flowing (∼1 l min^{-1}). This first experiment opened the way to a systematic investigation of the electronic structure of the active centre of haem proteins in physiological solutions using Fe L-edge spectroscopy. In this article , we present the Fe $L_{2,3}$-edge spectra of beef liver catalase in physiological solutions, which show a similar HS state to metHb but also clear differences from it.[2] We also report on temperature effects, which are weak and reflect the near lack of dependence on enzyme activity.[13–15] The experimental procedures and methods are given in the ESI.†

2. Experimental and calculation details

2.1 X-Ray fluorescence yield measurements

The catalase samples (in the resting ferric form) from beef liver were prepared with a buffer of 50 mM KH_2PO_4, with the pH adjusted to 7.0 at 25 °C using 1 M KOH so as to approach physiological conditions. Details about the set up have been discussed in detail before.[2,23] The sample temperature was varied from 5 up to 30 °C. Higher temperatures (up to 37 °C) showed no changes in the spectrum. To minimize radiation damage, the sample was flowed through a cell equipped with a soft X-ray transparent silicon nitride (Si_3N_4) membrane window (500 × 500 nm^2), ensuring its renewal every ∼5 ms for a beam focus of 20 × 40 μm^2. The obtained spectra were normalized by dividing them by the current obtained from the refocus mirror of the BESSY II U41-PGM beamline just before the light entered the experimental setup.

2.2 Charge-transfer multiplet calculations

Quantitative information about bonding, back-bonding, charge-transfer and spin character could be obtained by modelling the XA spectra using charge-transfer multiplet theory,[17,20,24] which has proven its validity in interpreting transition metal L-edge spectra in systems such as molecules, condensed matter and proteins. Briefly, the theory begins with the Hamiltonian of the metal atom, taking into account all Coulomb interactions, as well as spin–orbit coupling between the atomic orbitals. To describe the local symmetry, ligand field parameters are added. The local symmetry of the iron sites in all haem species (either five-coordinated pyramidal or six-coordinated planar) is close to D_{4h} symmetry[25] and can be described starting from O_h symmetry.[26] In O_h symmetry, the 3d orbitals are split into t_{2g} (d_{xz}, d_{xy}, d_{yz}) and e_g (d_{z^2}, $d_{x^2-y^2}$) classes, with an energy difference of 10Dq. In lowering the symmetry from O_h to D_{4h}, the orbitals decompose into b_{2g} (d_{xy}), e_g (d_{xz}, d_{yz}), a_{1g} (d_{z^2}) and b_{1g} ($d_{x^2-y^2}$), and two more parameters (Ds and Dt) are introduced. The calculated spectra are broadened with a Lorentzian and a Gaussian to describe the lifetime and instrumental broadening, respectively. The ligand field parameters (10Dq, Ds and Dt) are adjusted to obtain the best fit to the experimental XAS spectra, however, Ds and Dt hardly influence them and can be set to zero.

Covalent mixing of the metal valence d-orbitals with the ligand valence p-orbitals is simulated using a charge-transfer model, which in the case of LMCT adds a $d^{n+1}\underline{L}$ configuration above the d^n ground state. The $d^{n+1}\underline{L}$ configuration is set at an energy Δ_{LM} above the d^n configuration, and these two states are coupled by a configuration interaction (CI), represented by the mixing term $T_i = \langle d^n|h|d^{n+1}\underline{L}\rangle$, where h is the molecular Hamiltonian and T_i is proportional to metal–ligand overlap for each of the i symmetry blocks. For a donor ligand system, the ground and LMCT states are written as linear combinations of $|3d^n\rangle$ and $|3d^{n+1}\underline{L}\rangle$ wavefunctions, while the L-edge excited state is a linear combination of $|2p^53d^{n+1}\rangle$ and $|2p^53d^{n+2}\underline{L}\rangle$ wavefunctions. The coefficients of these linear combinations are functions of T and Δ_{LM} for the ground state, and T' and Δ_{LM}' for the excited state, where $\Delta_{LM}' = \Delta_{LM} + U - Q$ (also called the charge-transfer energy), with U being the 3d–3d electron repulsion (so-called Hubbard energy) and Q being the 2p–3d repulsion (core hole energy). Ligand field, T and Δ_{LM} are allowed to vary in the final state (*i.e.*, decrease) but have little effect on the covalent mixing, as was also found in ref. 19. Δ_{LM}' and $U - Q$ affect the energy position of the L_3- and L_2-edges. In order to include back-bonding (MLCT) in addition to σ-donation, it is necessary to introduce a third state, at Δ_{ML} above the d^n configuration. The ground-state

Table 1 Ground state configuration and charge-transfer multiplet parameters considered to reproduce experimental XA spectra associated to methaemoglobin and catalase at the Fe $L_{2,3}$-edges

Ground state configuration	Methaemoglobin 64% d^5 + 36% $d^6\underline{L}$	Catalase (LMCT) 63% d^5 + 37% $d^6\underline{L}$	Catalase (MLCT) 56% d^4L^- + 44% d^5	Catalase (LMCT + MLCT) 3% d^4L^- + 62% d^5 + 35% $d^6\underline{L}$
10Dq/eV	1.3	1.0	1.5	1.0
Δ_{LM}/eV	0	0	0	0
Δ_{ML}/eV	0	0	−2.0	−2.0
$U - Q$/eV	−2.0	−2.0	−1.0	−1.0
$T(b_{1g}$, MLCT)	0	0	1.4	0
$T(a_{1g}$, MLCT)	0	0	1.4	0
$T(b_{2g}$, MLCT)	0	0	0.7	0.7
$T(e_g$, MLCT)	0	0	0.7	0.7
$T(b_{1g}$, LMCT)	4.0	4.0	0	4.0
$T(a_{1g}$, LMCT)	3.2	2.8	0	2.8
$T(b_{2g}$, LMCT)	1.0	1.0	0	1.0
$T(e_g$, LMCT)	1.5	2.0	0	2.0

wavefunction becomes a linear combination of three configurations, $3d^{n-1}\underline{L}$, $3d^n$ and $3d^{n+1}\underline{L}$. By introducing MLCT parameters, $U - Q$ has to be changed in order to maintain good agreement with experimental spectra. This optimization was performed by switching off the MLCT mixing parameters and varying only Δ_{ML} and $U - Q$. Further details for the three configuration simulations, including both LMCT and MLCT, are given in refs. 18 and 19. For present purposes, the only parameters of relevance are the cubic ligand field 10Dq, Δ_{LM}, Δ_{ML}, $U - Q$ and the mixing terms T_i (Table 1).

3. Results

3.1 Experimental observations

Fig. 1a and b show the Fe $L_{2,3}$-edge spectra of metHb and catalase; obvious differences are seen between them. The L_3-edge feature exhibits a doublet in both cases, but the low energy band is almost three times weaker relative to the main peak in catalase than in metHb, while the energy difference between the two peaks is identical. As already discussed,[2,19] the first component is due to transitions from the p-core orbital to the valence d_{xy}, d_{yz} and d_{xz} orbitals, while the second is due to transitions to the $d_{x^2-y^2}$ and d_{z^2} orbitals. The similar energy splitting in both systems shows that, just as for metHb,[2] catalase is in a high spin (HS) state. The decreased intensity of the low energy feature may suggest a larger occupancy of the d_{xy}, d_{yz} and d_{xz} orbitals in catalase, but as shown below, its origin is different. The ratio of integrated intensities between the L_3 and L_2 transitions deviates from 2 : 1 in the single-particle description, and is 1.7 for metHb and 1.5 for catalase. The deviation comes from the contribution of 3d–3d and 2p–3d correlation effects,[17] and the different ratio in the two systems reflects a change of correlation within the 3d valence band, itself resulting from a change of electronic structure.

The temperature dependence of the spectrum is shown in Fig. 2. While the pre-edge feature at the L_3-edge does not change much in intensity, a weak but systematic increase (by about 10%) with temperature is observed for the main peak (711 eV). The integrated intensity over the whole spectral range of both edges increases but only weakly. The weak temperature effect observed here is in agreement with the almost temperature-independent activity of catalase previously reported.[13–15]

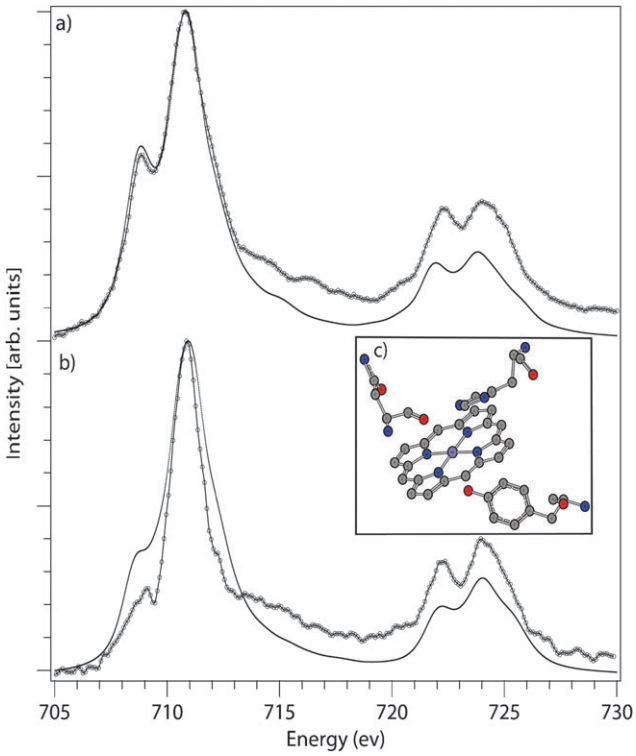

Fig. 1 The experimental Fe $L_{2,3}$-edge X-ray absorption near edge structure (XANES) of the Fe^{3+} centre of (a) the methaemoglobin and of (b) the beef liver catalase under near physiological conditions (1 mM concentration aqueous solution at pH 7.0 and T = 30 °C). The simulated Fe $L_{2,3}$-edge spectra of methaemoglobin and catalase are presented as a solid line under each experimental spectrum (see text for details). (c) The active centre of the catalase presented schematically.

3.2 Charge-transfer in catalase and metHb

In order to extract more quantitative information from the XA spectra of metHb and catalase, we performed charge-transfer multiplet calculations. These spectra have been found to be better reproduced by considering an initial Fe(III) ground state, in accordance with the expected oxidation state of Fe in the prepared sample (see section 2.1). Thus, $\Delta_{LM} = E(3d^5) - E(3d^6\underline{L})$ and $\Delta_{ML} = E(3d^4\underline{L}^-) - E(3d^5)$, where $E(X)$ represents the energy of the X configuration.

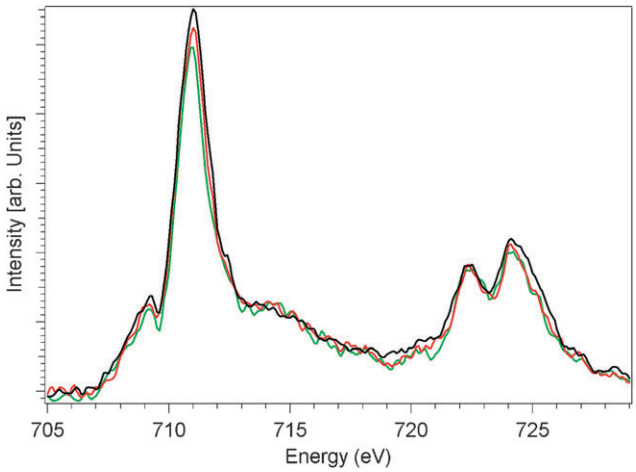

Fig. 2 Fe $L_{2,3}$-edge spectra of catalase at different temperatures: 5 °C (green), 15 °C (red) and 30 °C (black).

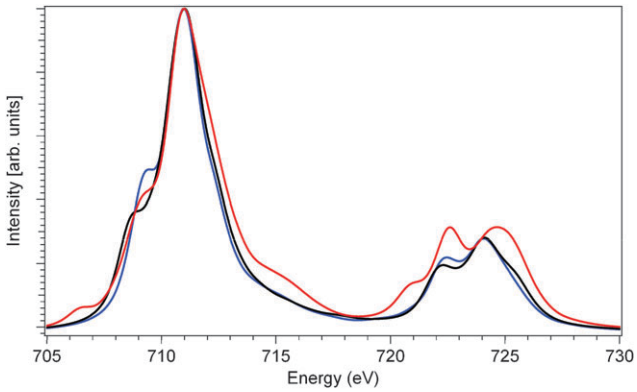

Fig. 3 Simulated Fe $L_{2,3}$-edge spectra of catalase with LMCT contributions only (blue), MLCT (red) and with both LMCT and MLCT contributions (black).

Hocking *et al.*[18,19] have carried out a detailed analysis of the L-edge spectra of a low spin (LS) ferric porphyrin, which has served as a basis for our simulation of the $L_{2,3}$-edge absorption spectrum of metHb,[2] as reproduced in Fig. 1a (see Table 1 for the multiplet parameters). It was shown in ref. 19 that there is significant charge-transfer from the porphyrin to the metal (LMCT) in ferric haem systems, and this was supported by density functional theory (DFT) calculations.[19] We therefore used the same LMCT parameters as a starting point for our simulations, even though the spin state is different for our samples. Table 1 shows that for metHb, the final parameters are similar to those of ref. 19. In this case, no MLCT contributions need to be included to obtain a good agreement between the experimental and simulated spectra.

For catalase, we proceeded in a stepwise fashion. We first performed simulations with only ligand–metal charge-transfer (LMCT, $3d^6\underline{L}$), but this turned out to be insufficient, and we therefore added metal–ligand charge-transfer (MLCT, $3d^4\underline{L}^-$). We expected that the $T(e_g$, LMCT) and $T(a_{1g}$, LMCT) parameters, accounting for the mixing between ligand orbitals and the d_{xz}/d_{yz} and d_{z^2} metal orbitals, respectively, would be affected because these metal orbitals are the most modified by the substitution of the proximal ligand in going from metHb to catalase. These parameters influence the relative intensity of the pre-edge peak compared to the main peak, and also the energy splitting between peaks at the L_2-edge. However, a variation of $T(e_g$, LMCT) only induces a marked shift of the peak close to 722 eV, and can deteriorate strongly the line shape of the XA spectrum. This allows the determination of a reasonable balance between these two parameters to reliably reproduce the experimental data. Fig. 3 presents the calculated XA spectrum including only LMCT. It contains all the main experimentally observed transitions at the $L_{2,3}$-edges, namely those at about 709, 711, 722 and 724 eV, with relative intensities in accordance with XA measurements (Fig. 1b). However, the peak at 709 eV appears too intense and should be attenuated by adding back-bonding *via* MLCT. This is realized by increasing the mixing parameters $T(b_{2g}$, MLCT) and $T(e_g$, MLCT), which are the only ones that significantly improve the agreement between the calculations and the experimental spectra. This latter point is consistent with the fact that the π-delocalization is expected to lead to different reactivities of catalase and metHb, since these parameters are related to the d_{xy} and d_{xz}/d_{yz} orbitals.[19]

It is important to stress that MLCT alone is unable to reproduce the experimental observations. Fig. 3 shows a typical spectrum including MLCT only (see Table 1 for the corresponding multiplet parameters). It shows pronounced transitions at 706.5 and 721 eV, in disagreement with the experimental spectra. These peaks stem from σ back-donation resulting from the rise of the $T(b_{1g}$, MLCT) and $T(a_{1g}$, MLCT) mixing terms. Therefore, in order to make these peaks disappear, σ back-donation must be reduced. However, this procedure degrades the whole L_2-edge and weakens the intensity of the transition at about 709 eV, which is a major feature of the XA spectrum of catalase. Hence, MLCT alone cannot explain the experimental observations. In fact, only 3% of the $d^4\underline{L}^-$ MLCT configuration should be introduced in the ground state (Table 1) to reduce the intensity of the pre-edge peak at the L_3-edge, obtained by means of a calculation including only LMCT. Such sensitivity due to the addition of MLCT has already been observed in a solid state molecular material at the Co $L_{2,3}$-edges,[27] but this is the first time that it has been observed at the Fe $L_{2,3}$-edges of a haem protein in a physiological solution. In addition, this reveals that XAS is able to probe very efficiently the electronic structure and shed light on even weak charge-transfer effects in metal-based molecular complexes.

The crystal field parameters used for metHb and catalase are almost the same, but modifications can be identified in the LMCT properties for the mixing between ligand orbitals and the $3d_{z^2}$ metal orbital, on the one hand, and the $3d_{xz}/3d_{yz}$ orbitals, on the other. The variation of the former reflects mainly the difference in σ donation from the axial tyrosine to the Fe(III) metal ion. In contrast, the slight increase of the latter suggests a weak rise in π-donation, mainly from the axial tyrosine to the metal. In the event of the porphyrin being the principal contributor, an additional gain in π-donation to the d_{xy} metal orbital would have been expected, but was not observed. Note that in our simulation, only π back-donation to the porphyrin and the axial tyrosine has been introduced.

Adding σ back-donation does not improve the quality of the simulation. Thus, the intensity decrease of the L_3 pre-edge feature is not due to an increased occupancy of the $d(e_g, b_{2g})$ orbitals, but rather it results from the stronger delocalization of orbitals (decreased d-character), which reduces the overlap with the initial p-core orbital.

4. Discussion

In metHb, π back-donation was found to be much less effective than in LS iron porphyrins because of its HS state.[2] Catalase is also in the HS state but the situation is different. Understanding the degree and origin of the π-delocalization of haem systems has important implications for describing their reactivity. The fast electron transfer rates in proteins are facilitated by coupling through either hole or electron super exchange pathways, which enhance the interactions between donor and acceptor redox sites.[19,28] For a super exchange mechanism to be efficient, the redox-active molecular orbitals must have sufficient delocalization through the protein. Recalling that catalase has the highest turnover numbers of all enzymes,[1] π-delocalization is expected to be much stronger in catalase than in metHb. In our case, the stronger π-donation of the ligands to the d_{xy} and d_{yz} holes of the Fe(III) site favours a stronger hole super exchange mechanism, and the noticeable π back-donation of the Fe(III) d-orbitals to the ligands facilitates an electron super exchange mechanism.

According to our study, the most likely cause of the different electronic structures of catalase and metHb is the substitution of the proximal ligands. In catalase, the proximal tyrosine binds to the Fe atom *via* a phenolic oxygen atom at ~2.0 Å, which itself is hydrogen-bonded to two N atoms of an Arg residue. The increased reactivity of catalase is due to back-donation to the phenolic oxygen. This confers the partial ferryl character to its metal atom. As far as temperature effects are concerned, and because the partial ferryl character of the centre stems from the proximity of the distal tyrosine, we believe that the latter should cause the subtle changes observed in the spectra, and therefore in the electronic structure. Thermal motion of the tyrosine, or even the proximity of Arg (and other residues), may modulate the amount of π-back-bonding to the distal residue, causing the weak changes in the spectra.

One may ask if the electronic structure we determined here is sufficient to account for the activity of catalase compared to that of metHb. The role of the distal residues has been discussed by Fita and co-workers.[1,7] When peroxide enters the haem cavity, its possible orientation and binding site are very limited due to steric effects forcing the formation of a hydrogen bond to the Nε of His, and the electrostatic interaction with the Fe(III) (with its partial ferryl character, as we now have established) leads to lower pK_a values of the peroxide OH group, weakening its bond. At the same time, the second oxygen atom forms a hydrogen bond with His in such a way that a proton is transferred from the first oxygen to the second. The deprotonation of the former leads to the elongation and polarization of the O–O bond, which breaks as a peroxide oxygen, is coordinated to the Fe centre and then evolves into a Fe^{IV}=O moiety and a haem radical. This explanation, fully based on structural arguments, needs, however, to include the lack of a noticeable temperature effect on the enzymatic activity of catalase,[14,15] which seems to be supported by our L-edge spectra and the fact that this activity is present even below the dynamic transition observed for proteins.[13]

5. Conclusions

In this study, we have determined a clear difference between the electronic structure of the active metalloporphyrin centre of catalase and haemoglobin, which may explain their different biochemical activities. While much of the debate around biological functions focuses on geometric structural considerations, *e.g.* the nature and configuration of residues in the haem cavity, mainly obtained from X-ray crystallographic studies and site directed mutagenesis, the ability to perform soft X-ray studies of proteins in physiological environments brings a new element to the description of biological functions by unravelling the electronic structure of active centres, which are at the heart of biochemical activity.

Acknowledgements

We thank Dr R. Pietri for useful discussions. E. F. A. thanks the Swiss NSF for the grant IZKOZ2-126024 during his stay in Lausanne and the European Science Foundation DYNA programme for financial support.

References

1 P. Nicholls, I. Fita and P. C. Loewen, *Adv. Inorg. Chem.*, 2000, **51**, 51.
2 E. F. Aziz, N. Ottosson, S. Bonhommeau, N. Bergmann, W. Eberhardt and M. Chergui, *Phys. Rev. Lett.*, 2009, **102**, 68103.
3 J. Everse, K. E. Everse and M. B. Grisham, *Peroxidases in Chemistry and Biology*, CRC Press, Boca Raton, 1991, vol. I and II; C. Redaelli, E. Monzani, L. Santagostini, L. Casella, A. M. Sanangelantoni, R. Pierattelli and L. Banci, *ChemBioChem*, 2002, **3**, 226.
4 M. Chance, L. Powers, C. Kumar and B. Chance, *Biochemistry*, 1986, **25**, 1259.
5 T. L. Poulos and J. Kraut, *J. Biol. Chem.*, 1980, **255**, 8199.
6 B. Chance, A. Naqui, C. Kumar, L. Powers and Y. Ching, *Fed. Proc.*, 1985, **44**, 676.
7 I. Fita and M. G. Rossmann, *J. Mol. Biol.*, 1985, **185**, 21.
8 L. Powers, A. Hillar and P. C. Loewen, *Biochim. Biophys. Acta, Protein Struct. Mol. Enzymol.*, 2001, **1546**, 44.
9 H. P. Hersleth, U. Ryde, P. Rydberg, C. H. Gorbitz and K. K. Andersson, *J. Inorg. Biochem.*, 2006, **100**, 460.
10 R. K. Behan and M. T. Green, *J. Inorg. Biochem.*, 2006, **100**, 448.
11 M. Newcomb, J. A. Halgrimson, J. H. Horner, E. C. Wasinger, L. X. Chen and S. G. Sligar, *Proc. Natl. Acad. Sci. U. S. A.*, 2008, **105**, 8179.
12 O. Horner, J. M. Mouesca, P. L. Solari, M. Orio, J. L. Oddou, P. Bonville and H. M. Jouve, *JBIC, J. Biol. Inorg. Chem.*, 2007, **12**, 509.
13 J. M. Bragger, R. V. Dunn and R. M. Daniel, *Biochim. Biophys. Acta, Protein Struct. Mol. Enzymol.*, 2000, **1480**, 278.
14 X. L. Shi, M. Q. Feng, Y. J. Zhao, X. Guo and P. Zhou, *Biotechnol. Lett.*, 2007, **30**, 181.
15 J. Haber, P. Maslakiewicz, J. Rodakiewicznowak and P. Walde, *Eur. J. Biochem.*, 1993, **217**, 567.
16 E. I. Solomon, T. C. Brunold, M. I. Davis, J. N. Kemsley, S. K. Lee, N. Lehnert, F. Neese, A. J. Skulan, Y. S. Yang and J. Zhou, *Chem. Rev.*, 2000, **100**, 235; E. C. Wasinger, F. M. F. de Groot,

B. Hedman, K. O. Hodgson and E. I. Solomon, *J. Am. Chem. Soc.*, 2003, **125**, 12894.
17 F. M. F. de Groot, *Coord. Chem. Rev.*, 2005, **249**, 31.
18 R. K. Hocking, E. C. Wasinger, F. M. F. de Groot, K. O. Hodgson, B. Hedman and E. I. Solomon, *J. Am. Chem. Soc.*, 2006, **128**, 10442.
19 R. K. Hocking, E. C. Wasinger, Y. L. Yan, F. M. F. de Groot, F. A. Walker, K. O. Hodgson, B. Hedman and E. I. Solomon, *J. Am. Chem. Soc.*, 2007, **129**, 113.
20 F. de Groot and A. Kotani, *Core Level Spectroscopy of Solids*, Taylor & Francis, New York, 2008.
21 A. Arcovito, M. Benfatto, M. Cianci, S. S. Hasnain, K. Nienhaus, G. U. Nienhaus, C. Savino, R. W. Strange, B. Vallone and S. Della Longa, *Proc. Natl. Acad. Sci. U. S. A.*, 2007, **104**, 6211.
22 B. Winter and M. Faubel, *Chem. Rev.*, 2006, **106**, 1176; E. F. Aziz, S. Eisebitt, F. de Groot, J. Chiou, C. Dong, J. Guo and W. Eberhardt, *J. Phys. Chem. B*, 2007, **111**, 4440; E. F. Aziz, N. Ottosson, M. Faubel, I. V. Hertel and B. Winter, *Nature*, 2008, **455**, 89; N. Ottosson, E. F. Aziz, H. Bergersen, W. Pokapanich, G. Ohrwall, S. Svensson, W. Eberhardt and O. Bjorneholm, *J. Phys. Chem. B*, 2008, **112**, 16642; I. Lauermann, T. Kropp, D. Vottier, A. Ennaoui, W. Eberhardt and E. F. Aziz, *ChemPhysChem*, 2009, **10**, 532.
23 E. F. Aziz, M. Freiwald, S. Eisebitt and W. Eberhardt, *Phys. Rev. B: Condens. Matter Mater. Phys.*, 2006, **73**, 75120; E. F. Aziz, A. Zimina, M. Freiwald, S. Eisebitt and W. Eberhardt, *J. Chem. Phys.*, 2006, **124**, 114502; E. F. Aziz, W. Eberhardt and S. Eisebitt, *Z. Phys. Chem.*, 2008, **222**, 727; E. F. Aziz, S. Eisebitt, W. Eberhardt, L. Cwiklik and P. Jungwirth, *J. Phys. Chem. B*, 2008, **112**, 1262.
24 B. T. Thole, G. Vanderlaan, J. C. Fuggle, G. A. Sawatzky, R. C. Karnatak and J. M. Esteva, *Phys. Rev. B: Condens. Matter*, 1985, **32**, 5107.
25 T. Takano, *J. Mol. Biol.*, 1977, **110**, 569; S. E. V. Phillips, *J. Mol. Biol.*, 1980, **142**, 531.
26 A. B. P. Lever, *Inorganic Electronic Spectroscopy*, Elsevier, Amsterdam and New York, 2nd edn, 1984.
27 S. Bonhommeau, N. Pontius, S. Cobo, L. Salmon, F. M. F. de Groot, G. Molnár, A. Bousseksou, H. A. Dürr and W. Eberhardt, *Phys. Chem. Chem. Phys.*, 2008, **10**, 5882.
28 M. D. Newton, *Chem. Rev.*, 1991, **91**, 767; H. B. Gray and J. R. Winkler, *Annu. Rev. Biochem.*, 1996, **65**, 537.

